

Inhibition of T-type calcium channels protects neurons from delayed ischemia-induced damage.

²I. Nikonenko*, ¹M. Bancila*, ¹A. Bloc, ²D. Muller, ¹Ph. Bijlenga

¹Département des Neurosciences Cliniques, Hôpital Universitaire de Genève CH 1211
Genève 14, Suisse

²Département des Neurosciences Fondamentales, Centre Médical Universitaire CH 1211
Genève 4, Suisse

* These authors contributed equally to the work.

Running title: **Neuroprotection by T-type Ca²⁺ channels inhibition**

Corresponding Author:

Dr Philippe Bijlenga

Neurochirurgie, Hôpital Universitaire de Genève

24 rue Micheli-du-Crest

1211 Geneva 14, Switzerland

e-mail: philippe.bijlenga@hcuge.ch

Pages: 21

References: 37

Figures: 3

Abstract: 174 words

Introduction: 536 words

Discussion: 978 words

Abbreviations:

BAPTA-AM - 1,2-Bis(2-aminophenoxy)ethane-N,N,N',N'-tetraacetic acid tetrakis
(acetoxymethyl ester)

eGFP – enhanced green fluorescent protein

EGTA - Ethylene glycol-bis(2-aminoethylether)-N,N,N',N'-tetraacetic acid

FITC - fluoresceineisothiocyanate

HEK-293T - human embryonic kidney cells

K_{ATP} - ATP sensitive potassium channels

K_{dr} - delayed rectifier potassium channels

LVAs - low voltage activated calcium channels

OGD - oxygen-glucose deprivation

TRITC – tetramethylrhodamineisothiocyanate

Abstract

Intracellular calcium increase is an early key event triggering ischemic neuronal cell damage. The role of T-type voltage gated calcium channels in the neuronal response to ischemia has however never been studied. Using an in vitro model of ischemia-induced delayed cell death in rat organotypic hippocampal slice cultures we show that T-type calcium channels inhibitors drastically reduce ischemic cell damage. Immunostaining studies reveal the existence of $Ca_v3.1$ and $Ca_v3.2$ types of low-voltage-activated calcium channels in rat organotypic hippocampal cultures. Low extracellular calcium (100 nM) or increase of intracellular calcium buffering ability by BAPTA-AM significantly reduced ischemia-induced neuronal damage. Pharmacological inhibition of the T-type calcium current by mibefradil, kurtoxin, nickel, zinc and pimozide during the oxygen-glucose deprivation episode provided a significant protection against delayed neuronal death. Mibefradil and nickel exerted neuroprotective effects not only if administrated during the oxygen-glucose deprivation episode, but also in conditions of post-ischemic treatment. These data point to a role of T-type calcium currents in ischemia-induced, calcium-mediated neuronal cell damage and suggest a possible new pharmacological approach to stroke treatment.

Introduction

Ischemic neuronal damage remains a common cause of severe neurological disability and death thus making a search for neuroprotective drugs an extremely important issue. Among the early events in ischemia-induced cascades, extracellular calcium entry is of a critical importance as it triggers numerous mechanisms leading to cell damage and death (Fern, 1998; Nowicky and Duchen, 1998). Blocking of Ca^{2+} -permeable NMDA sensitive glutamate receptors markedly reduces the intracellular calcium rise in anoxia (Silver and Erecinska, 1990) and was shown to be neuroprotective in neuronal cell cultures (Choi, 1988) and in animal models of focal brain ischemia, hypoglycemia and trauma (Albers et al., 1989), but not in animal models of transient global ischemia (Buchan and Pulsinelli, 1990). Moreover, glutamate receptor antagonists revealed disappointing in clinical trials for acute treatment of brain ischemia because of significant side effects (Goldberg, 2005).

During ischemia, L-type voltage gated calcium channels also ensure an early intracellular calcium rise. Inhibiting L-type voltage gated calcium channels with dihydropyridine abolished the intracellular calcium rise usually observed after 2-4 minutes. No effect however was detected on a small very early intracellular calcium concentration increase (Pisani et al., 1998). Phase III clinical trials on L-type calcium channels inhibitors all concluded no efficacy (Goldberg, 2005).

The role of low voltage activated calcium channels (LVAs) during brain ischemia has never been studied. Low voltage activated calcium channels constitute a family of three types of calcium channels commonly referred to as T-type calcium channels: $\alpha 1\text{G}$ or $\text{Ca}_v3.1$, $\alpha 1\text{H}$ or $\text{Ca}_v3.2$, $\alpha 1\text{I}$ or $\text{Ca}_v3.3$ (for review see Perez-Reyes, 2003). Most brain regions express more than one isoform, and some neurons like olfactory granule cells and hippocampal pyramidal neurons express all three genes (Craig et al., 1999; Kase et al., 1999; Talley et al., 1999). An interesting property of T-type calcium channels is the possibility to sustain a continuous

calcium influx in neurons and glia at rest by a window current mechanism. The activation and inactivation curves of T-type calcium channels overlap and cross around -60mV. For this reason, a fraction of the channels cycle through all molecular conformations when the membrane potential ranges from -80 to -40mV. Therefore, when neurons are at rest, there is continuously a small fraction of channels that are open and sustain a tiny continuous calcium entry. This property has been shown to produce input signal amplification and bistability in thalamocortical neurons (Williams et al, 1997). It is implicated in the differentiation of myoblasts (Bijlenga et al., 2000), neuroendocrine differentiation of human prostate cancer cells (Mariot et al., 2002) and steroidogenesis in adrenal glomerulosa cells (Cohen et al., 1988; Rossier et al., 1998). Overexpression of T-Type calcium channels in HEK-293 cells has been shown to increase the intracellular calcium concentration (Chemin et al.2000). The early intracellular calcium concentration increase observed after initiation of an ischemic insult could be the expression of a change in equilibrium between the calcium influx, through T-type calcium channels, and efflux sustained by active mechanisms that dysfunction under metabolic stress.

In the present study we describe the neuroprotective effects of various LVAs inhibitors in a model of *in vitro* ischemia on rat organotypic hippocampal cultures. These observations support the hypothesis of a critical role for the T-type calcium “window” current during ischemic insult.

Materials and Methods

Immunostaining of transfected HEK-293T cells and hippocampal organotypic cultures

Human embryonic kidney cells (HEK-293T) were transfected as previously described (Chemin et al., 2001) using 2.7 µg of different pBK-CMV plasmid constructs that encode for Cav3.1 (Chemin et al., 2001), and Cav3.2 (Cribbs et al., 1998). In some experiments, the cells

were co-transfected with 0.3 μ g of pBB14 plasmid encoding the reporter gene for enhanced green fluorescent protein (eGFP; Brideau et al., 1998) to make transfected cells visible by fluorescence. Two days later, cells were harvested and plated on the sterile coverslips. One day later, cells were fixed for 10 min at 4°C in 4% paraformaldehyde (PAF) in PBS, preincubated in PBS with 10% fetal calf serum (Gibco, USA) (FCS) and 0.3% Triton X100 for 30 min and incubated with rabbit polyclonal anti-Ca_v3.1 or anti-Ca_v3.2 antibodies (1:500) (Brueggemann et al, 2005) kindly supplied by Dr L. Cribbs (Loyola University Medical Center, Maywood, Illinois), for 24 hours at 4°C. Secondary TRITC or FITC-labeled goat anti-rabbit IgG antibodies (Chemicon, USA, 1:100 in PBS containing 10% FCS) were applied for 2h at room temperature (RT). Cell nuclei were revealed by Hoescht staining (Sigma, Germany, 0.5mg/ml, 5 min at RT), and the cells were mounted onto Superfrost slides with FluorSave (Merck, USA). Hippocampal organotypic slices were fixed by immersion in 4% PAF solution for 30 min at 4°C and processed for Ca_v3.1 or Ca_v3.2 immunostaining as described above.

Oxygen-glucose deprivation experiments in organotypic hippocampal slice cultures.

Organotypic hippocampal slice cultures were prepared from 7 day old rats and maintained for 11-12 days in culture before the experiments (Stoppini et al., 1991). Ischemic insult was performed in an interface-type chamber as described (Bancila et al., 2004). Briefly, after placing the cultures in the chamber, oxygen-glucose deprivation (OGD) was produced by filling the chamber with a gas mixture containing 95% N₂ and 5% CO₂ and perfusing with a medium containing sucrose instead of glucose (in mM: 124 NaCl, 1.6 KCl, 2.5 CaCl₂, 1.5 MgCl₂, 24 NaHCO₃, 1.2 KH₂PO₄, 10 sucrose, and 2 ascorbic acid, pH 7.4, temperature 32°C) during 10 min (in the text, the term “ischemia” is also applied to this experimental condition). Except for the condition where post-ischemic effects of mibefradil and nickel were tested, all the drugs were always applied 5 minutes before (to insure diffusion of drugs

into cultures) and during the OGD episode. After the challenge, the cultures were placed back in the incubator for recovery in the usual culture medium. To study post-ischemic protection by mibefradil or nickel, drugs were added to the culture medium either just after, or 3 hours, or 6 hours after the OGD insult and maintained in the medium throughout the whole post-ischemia period.

A few hours before OGD experiments, organotypic slices were transiently treated with propidium iodide (PI, Sigma; 5 µg/ml, 20 min incubation) and observed in a fluorescence microscope (Axioscop 2, Zeiss, Germany) to assess cell viability. Only cultures exhibiting no or very low PI labeling at that stage were selected for the experiments. After the OGD, PI staining was carried out again at 2, 24 and 48 hours, to assess the timing and degree of ischemia-induced cell damage. In all experimental groups and at all time-points, the images of PI staining were taken at the same magnification, exposure time and parameters of the digital camera (Axiocam, Zeiss, Germany). The images were analyzed by using Photoshop®7 software (Adobe Systems Inc.) (Bancila et al., 2004). Images of the whole hippocampal slice culture were taken and converted to gray scale. We then adjusted the contrast so that the fluorescence precisely matched the contours of labelled pyramidal cell nuclei and then summed the intensity values of all pixels. We verified that these values were proportional to the number of PI labelled nuclei as tested by direct visual counting on specific samples. The result obtained for each slice was then normalized to the mean of 8 slice cultures exposed to OGD under control conditions within the same experiment. All fluorescence data were thus expressed as percent of a control value and then averaged across experiments. Statistical significance was assessed using the unpaired Student t-test.

Evoked transmission experiments in organotypic hippocampal slice cultures.

Slice cultures were placed in a recording chamber and continuously perfused with artificial cerebrospinal fluid containing (in mM) : 124 NaCl, 1.6 KCl, 1.2 KH₂PO₄, 24 NaHCO₃, 10

glucose, 2 ascorbic acid, pH 7.4, saturated with 95% O₂ / 5% CO₂. Stimulating and recording electrodes were positioned in CA1 stratum radiatum. Pair pulse evoked excitatory postsynaptic field potentials (EPSPs) were recorded before and during application of 10 μM mibefradil using an Axoclamp 2B (Axon instruments, Foster City, CA). Initial slopes and amplitudes of all EPSPs and ratios of pair pulse EPSPs amplitudes were calculated. Data obtained in the presence of mibefradil were expressed as percent of control baseline values. Statistical significance was assessed using the paired Student t-test.

Results

Experiments on HEK-293T expressing recombinant Ca_v3.1 or Ca_v3.2 channels have shown that about 50% of Hoescht labeled cells were stained using antibodies directed against Ca_v3.1 or Ca_v3.2 types of LVAs (Brueggemann et al, 2005) 24 hours after transfection. No immunostaining was observed in non-transfected HEK-293T cells (data not shown). No cross-staining was observed when using anti-Ca_v3.1 antibodies on Ca_v3.2 transfected HEK-293T or vice-versa (Fig. 1A-D). Thus, antibodies used in our experiments adequately revealed Ca_v3.1 and Ca_v3.2 types of LVAs. These antibodies, when applied to rat organotypic hippocampal cultures, clearly showed labeling in the dentate gyrus, CA3 and CA1 areas (Fig. 1E-F).

After exposure of organotypic hippocampal slice cultures to a transient (10 min) OGD episode, almost no cell death was observed 2 hours after the insult, while at 24 h and 48 h PI staining showed significant cell damage (Fig. 2, insets). Delayed cell death was usually observed in the CA1 area and, occasionally, in CA3 and DG regions, if the damage was massive. As revealed in the preliminary experiments by means of electron microscopy, the damage was predominantly attributed to neurons, while glial population was not impaired by this brief OGD episode. Even 30-45 min of OGD did not provoke glial cell death inside the

cultures, while neurons in all hippocampal areas showed in these conditions the signs of massive immediate death (data not shown). Thus, our *in vitro* ischemia model reproduces a delayed neuronal cell death similar to that observed in the penumbra region during stroke.

To check whether the induction of this delayed death was calcium dependent, we performed these experiments in conditions of low extracellular calcium (calcium-EGTA buffered at 100 nM calcium) or increased intracellular calcium buffer capacity with BAPTA-AM (10 μ M). In both cases we observed significant neuroprotection: less than 20% of propidium iodide fluorescence was detected at 48h compared to control cultures (100%) (Fig 2).

Application of the LVAs blocker mibefradil during the OGD insult at a concentration of 10 μ M protected the cultures very significantly, with 13 ± 5.5 % of PI fluorescence at 48h compared to untreated control cultures ($p < 0.002$). When tested in eGFP/ $Ca_v3.2$ co-transfected HEK cells, 10 μ M mibefradil reduced the calcium current by $93 \pm 2.7\%$ confirming that at this concentration of the drug the inhibition was almost complete (data not shown). Also, 10 μ M mibefradil applied to hippocampal slice cultures did not significantly affect evoked excitatory transmission and thus did not alter action potential-dependent synaptic mechanisms. Neither the slopes nor the amplitudes nor the ratio of paired pulse evoked excitatory postsynaptic field potentials were significantly affected by more than 15 minutes of mibefradil application ($93 \pm 6\%$; $98 \pm 5\%$; $106 \pm 8\%$ respectively $N=4-5$). At 1 μ M mibefradil concentration, the neuroprotective effect was reduced, but was still significant, with $39 \pm 11\%$ of propidium iodide fluorescence compared to controls ($p < 0.05$). No significant inhibition of the calcium current and no neuronal protection were observed with 0.2 μ M mibefradil, showing a clear dose-dependence of the effect. To confirm this, we further tested the effects of other LVAs blockers in our ischemia model. The neuroprotective effect of 350 nM and 500 nM kurtoxin applied during the OGD episode was very significant, with respectively $38 \pm 12\%$ and $10.4 \pm 3.2\%$ of PI fluorescence after the insult compared to control cultures.

Concurrently, we observed no effect on cell survival with application of 50 nM kurtoxin (Fig. 2). A strong protection was also obtained with 50 μ M nickel, 1 μ M zinc and, to a lesser amount, 1 μ M pimozone (respectively, $16\% \pm 6\%$, $23\% \pm 2\%$ and $35\% \pm 8\%$ of propidium iodide fluorescence 48h after the insult compared to controls) (Fig. 2). These doses of nickel and zinc were also effective in blocking $Ca_v3.2$ current recorded from eGFP/ $Ca_v3.2$ co-transfected HEK-293T cells (respectively, $85 \pm 3.6\%$ and $66 \pm 8.5\%$ inhibition, data not shown). We measured the effect of the inhibition of high voltage activated calcium channels with 10 μ M nifedipine on delayed neuronal death in the same conditions as used when inhibiting low voltage activated calcium channels. In this case, no significant reduction of PI fluorescence was observed ($84 \pm 22\%$, data not shown).

Interestingly, mibefradil at a concentration of 10 μ M or nickel at a concentration of 50 μ M were also neuroprotective if applied not during the insult, but immediately after and during the remaining 48h of the experiment. Compared to control cultures, PI fluorescence at 48h was reduced to $21 \pm 5\%$ in mibefradil-treated cultures and to $19 \pm 3\%$ in nickel-treated cultures ($p < 0.05$). A smaller but still significant protective effect was also observed when mibefradil or nickel were added to the culture medium 3 hours after the OGD insult, with $53 \pm 10\%$ and $60\% \pm 15\%$ of PI fluorescence at 48h respectively ($p < 0.03$). However, no significant protection was observed when mibefradil treatment was started six hours after the OGD episode (Fig. 3).

Discussion

Much evidence indicates that a small and slow intracellular calcium concentration increase takes place during the early phase corresponding to the first 2 to 3 minutes of ischemia. It starts just after cells transiently alkalinize secondarily to the hydrolysis of phosphocreatins (Silver and Erecinska, 1990). It has been observed *in vivo* and *in vitro* in acute hippocampal

slices and in dissociated neurons (Pisani et al., 1998). The origin of the calcium increase has been demonstrated to be extracellular, while intracellular and mitochondrial calcium stores seem not to be involved (Nowicky and Duchon, 1998). High voltage activated calcium channels have been proposed as a potential entry pathway for calcium, but application of dihydropyridine in animal studies (Silver and Erecinska, 1990) and in dissociated cortical neurons (Pisani et al., 1998) either did not modify the calcium concentration increase profile over time, or only acted on a delayed component.

Low voltage activated calcium channels have been suggested to be an important factor for intracellular glial calcium increase and cell death during ischemia in neonatal rat optical nerve white matter (Fern, 1998). The aim of the present study was to evaluate the effect of inhibition of T-type calcium current on delayed post-ischemic neuronal death in hippocampal neurons.

In rat hippocampal organotypic cultures used in our *in vitro* ischemia model, low voltage activated calcium channels $Ca_v3.1$ and $Ca_v3.2$ are indeed expressed in CA1, CA3 and dentate gyrus areas, as shown by immunocytochemistry. The fact that significantly less neurons suffer delayed neuronal death when exposed to low extracellular calcium or after increasing the intracellular calcium buffering ability during the OGD insult confirms the calcium-dependence of delayed cell death and correlates with earlier observations (Abdel-Hamid and Tymianski, 1997).

In resting neurons and glia, the intracellular calcium concentration is maintained by the equilibrium between a constant passive calcium influx and an energy-consuming pumping. T-type voltage gated calcium channels sustain a small but constant calcium current at membrane potential between -80 and -40 mV (Bijlenga et al 2000). At rest, neurons and glia are hyperpolarized close to -70 mV. We expect that in resting neurons and glia calcium continuously flows in through voltage activated T-type calcium channels. During ischemia,

the metabolic resources are challenged and we hypothesize that calcium extrusion is affected. Reducing or abolishing the calcium influx would be beneficial by itself, and would also spare energy for other essential house keeping cellular activities. In line with this hypothesis, we show here that pharmacological inhibition of the T-type calcium current by LVAs blockers mibefradil, kurtoxin, nickel, zinc and pimozide at effective concentrations that inhibit more than 80% of the current provides a very significant protection against delayed neuronal death. All these drugs are selective LVAs inhibitors, although most of them have additional effects. Mibefradil was described as a first selective T-type calcium current blocker (Clozel et al., 1997), but it has been also shown to block delayed rectifier potassium channels (K_{dr}) at similar concentrations, to significantly inhibit L-type calcium channels (Liu et al., 1999) and block in a state-dependent manner sodium channels (McNulty and Hanck 2004). The effects observed here are however unlikely to be due to a block of sodium channels, since it could be reproduced by all other calcium channel antagonists used and since mibefradil did not significantly affect evoked action potential-dependent synaptic transmission under those conditions. Among other blockers tested, at the concentration used in our experiments, nickel is a traditional T-type calcium current blocker (Hille, 2001). Other divalent metals like Cu^{2+} and Zn^{2+} have also been recently described to be selective T-type calcium inhibitors (Jeong et al., 2003). At small concentrations, as used in our experiments, zinc also activates ATP sensitive potassium channels (K_{ATP}) (Bancila et al., 2004; Bloc et al., 2000). Kurtoxin is a peptide purified from scorpion venom and was reported to bind with high affinity to $Ca_v3.1$ type LVAs and inhibit the T-type calcium current by modifying the channel gating. This toxin was shown to distinguish between T-type calcium channels and high voltage activated calcium channels (Chuang et al., 1998; Sidach and Mintz, 2002). At concentration of 350 nM, kurtoxin was reported to inhibit almost totally the current of $Ca_v3.1$ channels and 80% of $Ca_v3.2$ channels' current, while $Ca_v3.3$ type seems to be resistant (Olamendi-Portugal et al.,

2002). Recently pimoziide, a neuroleptic drug, has also been described to be a selective T-type calcium channel blocker with a half-inhibition concentration estimated at ~100 nM for all Ca_v3 channels, although $\text{Ca}_v3.2$ is less sensitive (Santi et al., 2002). It is 10 times more selective for LVAs than for high voltage activated calcium channels. To exclude the possibility that neuroprotective effect observed with LVAs inhibitors is in fact a non specific effect due to inhibition of high voltage activated calcium channels, we inhibited L-type calcium current with nifedipine and performed OGD. In our conditions we observed no significant protection against delayed neuronal death.

Recently Rekling (Rekling, 2003) reported the neuroprotective effect of anticonvulsants on organotypic hippocampal cultures subjected to transient ischemia. Interestingly, ethosuximide, phenobarbital and phenytoine reported to be the most neuroprotective anticonvulsants are also the drugs with the most potent T-type calcium current inhibitory activity (respectively $\text{EC}_{50} = 23,7\mu\text{M}$, $1,7\mu\text{M}$, $7,3\mu\text{M}$) (Todorovic and Lingle, 1998; Todorovic et al., 2000).

In spite of the different pharmacological profiles of the LVAs blockers tested, all of them act as potent T-type calcium current inhibitors, and all of them ensured significant neuroprotection after a transient OGD in our experiments. The converging neuroprotective effects of these various drugs which, at the concentrations used, exhibit selectivity for T-type calcium channels support the hypothesis suggesting an important role of LVAs in ischemia-induced cell damage. As the effect may not only be neuroprotective when the drugs are applied during the OGD episode, as shown with mibefradil and nickel, but also when applied shortly after the insult, these data open new perspectives of possible pharmacological approaches to neuroprotection.

Acknowledgments

We would like to thank Dr Leanne Cribbs for providing us the antibodies against Ca_v3.1 and Ca_v3.2, Dr Philippe Lory and Dr Edward Perez-Reyes for plasmid constructs with Ca_v3.1 and Ca_v3.2, and Marlis Moosmayer and Lorena Parisi-Jourdain for excellent technical assistance.

Reference List

Abdel-Hamid KM, Tymianski M (1997) Mechanisms and effects of intracellular calcium buffering on neuronal survival in organotypic hippocampal cultures exposed to anoxia/aglycemia or to excitotoxins. *J Neurosci* **17**: 3538-3553.

Albers GW, Goldberg MP, Choi DW (1989) N-methyl-D-aspartate antagonists: ready for clinical trial in brain ischemia? *Ann Neurol* **25**: 398-403.

Bancila V, Nikonenko I, Dunant Y, Bloc A (2004) Zinc inhibits glutamate release via activation of presynaptic KATP channels and reduces ischemic damage in rat hippocampus. *J Neurochem* **90**: 1243-1250.

Bijlenga P, Liu JH, Espinos E, Haenggeli CA, Fischer-Lougheed J, Bader CR, Bernheim L (2000) T-type alpha 1H Ca²⁺ channels are involved in Ca²⁺ signaling during terminal differentiation (fusion) of human myoblasts. *Proc Natl Acad Sci U S A* **97**: 7627-7632.

Bloc A, Cens T, Cruz H, Dunant Y (2000) Zinc-induced changes in ionic currents of clonal rat pancreatic -cells: activation of ATP-sensitive K⁺ channels. *J Physiol* **529** Pt 3: 723-734.

Brideau AD, Banfield BW, Enquist LW (1998) The Us9 gene product of pseudorabies virus, an alphaherpesvirus, is a phosphorylated, tail-anchored type II membrane protein. *J Virol* **72**: 4560-4570.

Brueggemann LI, Martin BL, Barakat J, Byron KL, Cribbs LL (2005) Low voltage-activated calcium channels in vascular smooth muscle: T-type channels and AVP-stimulated calcium spiking. *Am.J.Physiol Heart Circ.Physiol* **288**: H923-935.

Buchan A, Pulsinelli WA (1990) Hypothermia but not the N-methyl-D-aspartate antagonist, MK-801, attenuates neuronal damage in gerbils subjected to transient global ischemia. *J Neurosci* **10**: 311-316.

Chemin J, Monteil A, Briquaire C, Richard S, Perez-Reyes E, Nargeot J, Lory P (2000) Overexpression of T-type calcium channels in HEK-293 cells increases intracellular calcium without affecting cellular proliferation. *FEBS Lett* **478**: 166-172.

Chemin J, Monteil A, Bourinet E, Nargeot J, Lory P (2001) Alternatively spliced alpha(1G) (Ca(V)3.1) intracellular loops promote specific T-type Ca(2+) channel gating properties. *Biophys J* **80**: 1238-1250.

Choi DW (1988) Calcium-mediated neurotoxicity: relationship to specific channel types and role in ischemic damage. *Trends Neurosci* **11**: 465-469.

Chuang RS, Jaffe H, Cribbs L, Perez-Reyes E, Swartz KJ (1998) Inhibition of T-type voltage-gated calcium channels by a new scorpion toxin. *Nat Neurosci* **1**: 668-674.

Clozel JP, Ertel EA, Ertel SI (1997) Discovery and main pharmacological properties of mibefradil (Ro 40-5967), the first selective T-type calcium channel blocker. *J Hypertens Suppl* **15**: S17-S25.

Cohen CJ, McCarthy RT, Barrett PQ, Rasmussen H (1988) Ca channels in adrenal glomerulosa cells: K⁺ and angiotensin II increase T-type Ca channel current. *Proc Natl Acad Sci U S A* **85**: 2412-2416.

Craig PJ, Beattie RE, Folly EA, Banerjee MD, Reeves MB, Priestley JV, Carney SL, Sher E, Perez-Reyes E, Volsen SG (1999) Distribution of the voltage-dependent calcium channel alpha1G subunit mRNA and protein throughout the mature rat brain. *Eur J Neurosci* **11**: 2949-2964.

Cribbs LL, Lee JH, Yang J, Satin J, Zhang Y, Daud A, Barclay J, Williamson MP, Fox M, Rees M, Perez-Reyes E (1998) Cloning and characterization of alpha1H from human heart, a member of the T-type Ca²⁺ channel gene family. *Circ Res* **83**: 103-109.

Fern R (1998) Intracellular calcium and cell death during ischemia in neonatal rat white matter astrocytes in situ. *J Neurosci* **18**: 7232-7243.

- Goldberg M (2005) The Internet Stroke Center <http://www.strokecenter.org/>.
- Hille B (2001) *Ionic Channels of Excitable Membranes*. Sunderland, MA: Sinauer.
- Jeong SW, Park BG, Park JY, Lee JW, Lee JH (2003) Divalent metals differentially block cloned T-type calcium channels. *Neuroreport* **14**: 1537-1540.
- Kase M, Kakimoto S, Sakuma S, Houtani T, Ohishi H, Ueyama T, Sugimoto T (1999) Distribution of neurons expressing alpha 1G subunit mRNA of T-type voltage-dependent calcium channel in adult rat central nervous system. *Neurosci Lett* **268**: 77-80.
- Liu JH, Bijlenga P, Occhiodoro T, Fischer-Lougheed J, Bader CR, Bernheim L (1999) Mibefradil (Ro 40-5967) inhibits several Ca²⁺ and K⁺ currents in human fusion-competent myoblasts. *Br J Pharmacol* **126**: 245-250.
- Mariot P, Vanoverberghe K, Lalevee N, Rossier MF, Prevarskaya N (2002) Overexpression of an alpha 1H (Ca_v3.2) T-type calcium channel during neuroendocrine differentiation of human prostate cancer cells. *J Biol Chem* **277**: 10824-10833.
- McNulty MM, Hanck DA (2004) State-dependent mibefradil block of Na⁺ channels. *Mol.Pharmacol.* **66**: 1652-1661.
- Nowicky AV, Duchen MR (1998) Changes in [Ca²⁺]_i and membrane currents during impaired mitochondrial metabolism in dissociated rat hippocampal neurons. *J Physiol* **507** (Pt 1): 131-145.
- Olamendi-Portugal T, Garcia BI, Lopez-Gonzalez I, Van Der WJ, Dyason K, Ulens C, Tytgat J, Felix R, Darszon A, Possani LD (2002) Two new scorpion toxins that target voltage-gated Ca²⁺ and Na⁺ channels. *Biochem Biophys Res Commun* **299**: 562-568.
- Perez-Reyes E (2003) Molecular physiology of low-voltage-activated t-type calcium channels. *Physiol Rev* **83**: 117-161.

Pisani A, Calabresi P, Tozzi A, D'Angelo V, Bernardi G (1998a) L-type Ca^{2+} channel blockers attenuate electrical changes and Ca^{2+} rise induced by oxygen/glucose deprivation in cortical neurons. *Stroke* **29**: 196-201.

Rekling JC (2003) Neuroprotective effects of anticonvulsants in rat hippocampal slice cultures exposed to oxygen/glucose deprivation. *Neurosci Lett* **335**: 167-170.

Rossier MF, Burnay MM, Maturana A, Capponi AM (1998) Duality of the voltage-dependent calcium influx in adrenal glomerulosa cells. *Endocr Res* **24**: 443-447.

Santi CM, Cayabyab FS, Sutton KG, McRory JE, Mezeyova J, Hamming KS, Parker D, Stea A, Snutch TP (2002) Differential inhibition of T-type calcium channels by neuroleptics. *J Neurosci* **22**: 396-403.

Sidach SS, Mintz IM (2002) Kurtoxin, a gating modifier of neuronal high- and low-threshold Ca^{2+} channels. *J Neurosci* **22**: 2023-2034.

Silver IA, Erecinska M (1990) Intracellular and extracellular changes of $[\text{Ca}^{2+}]$ in hypoxia and ischemia in rat brain in vivo. *J Gen Physiol* **95**: 837-866.

Talley EM, Cribbs LL, Lee JH, Daud A, Perez-Reyes E, Bayliss DA (1999) Differential distribution of three members of a gene family encoding low voltage-activated (T-type) calcium channels. *J Neurosci* **19**: 1895-1911.

Todorovic SM, Lingle CJ (1998) Pharmacological properties of T-type Ca^{2+} current in adult rat sensory neurons: effects of anticonvulsant and anesthetic agents. *J Neurophysiol* **79**: 240-252.

Todorovic SM, Perez-Reyes E, Lingle CJ (2000) Anticonvulsants but not general anesthetics have differential blocking effects on different T-type current variants. *Mol Pharmacol* **58**: 98-108.

Williams SR, Toth TI, Turner JP, Hughes SW, Crunelli V (1997) The 'window' component of the low threshold Ca^{2+} current produces input signal amplification and bistability in cat and rat thalamocortical neurones. *J Physiol* **505** (Pt 3): 689-705.

Footnotes section

This work was supported by a grant from the Théodore Ott Fund for basic neurological research of the Swiss Academy of Medical Sciences.

Figure legends

Figure 1:

Immunocytochemistry using antibodies against $Ca_v3.1$ (column 1) and $Ca_v3.2$ (column 2).

A, B - $Ca_v3.1$ transfected HEK-293T cells. C, D - $Ca_v3.2$ transfected HEK-293T cells. Cell nuclei are blue (Hoechst staining); TRITC-labeled secondary antibodies were used (red staining). E, F – LVAs staining in organotypic hippocampal slices (FITC – labeled secondary antibodies). CA3 – CA3 pyramidal cell layer; DG – dentate gyrus. Inset: higher magnification in CA1 pyramidal layer. Scale bars: A-D, 10 μm ; E, F, 100 μm ; inset, 20 μm .

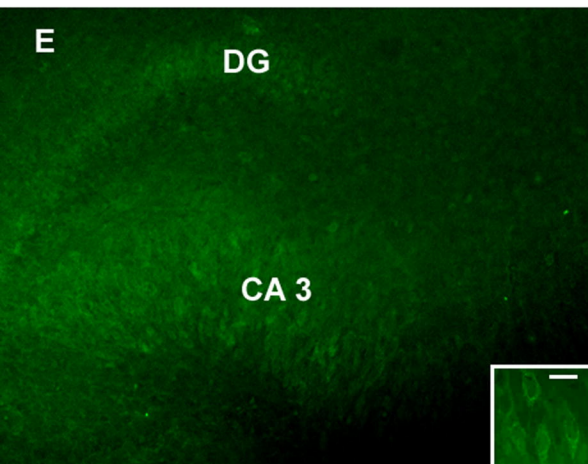
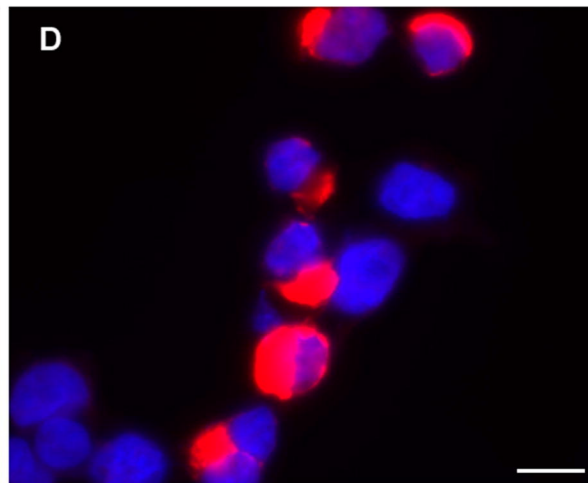
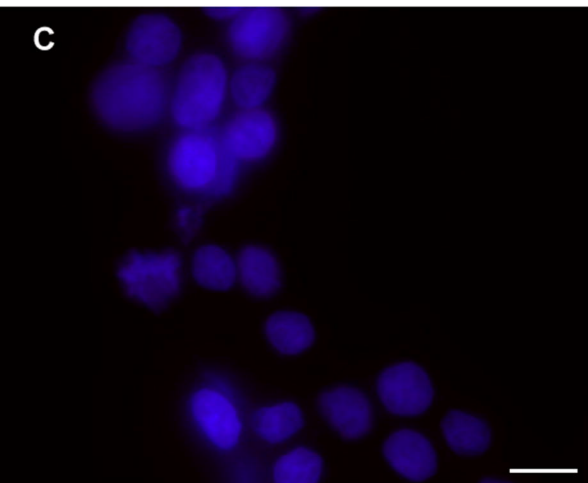
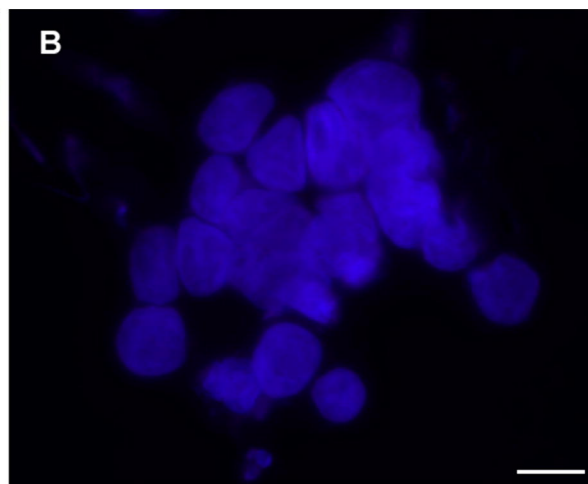
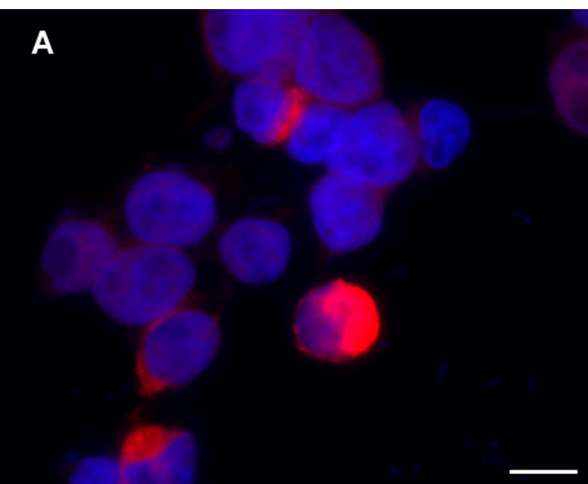
Figure 2:

Normalized propidium iodide fluorescence in organotypic hippocampal slices 48 hours after transient OGD in the presence of low extracellular calcium concentration (EGTA), increased intracellular calcium buffering ability (BAPTA) or various concentrations of mibefradil, kurtoxin, nickel, zinc and pimozone. Insets represent the examples of PI fluorescence images in organotypic hippocampal cultures 2h and 48h after insult in control condition and with 500 nM kurtoxin.

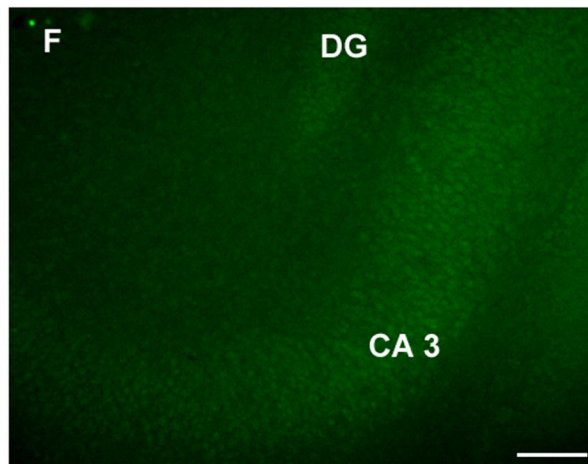
Figure 3:

Normalized PI fluorescence in organotypic hippocampal slices 48 hours after transient OGD: 10 μM mibefradil and 50 μM nickel treatment was applied either during OGD, or started at different times after the insult.

Figure 1



1



2

Figure 2

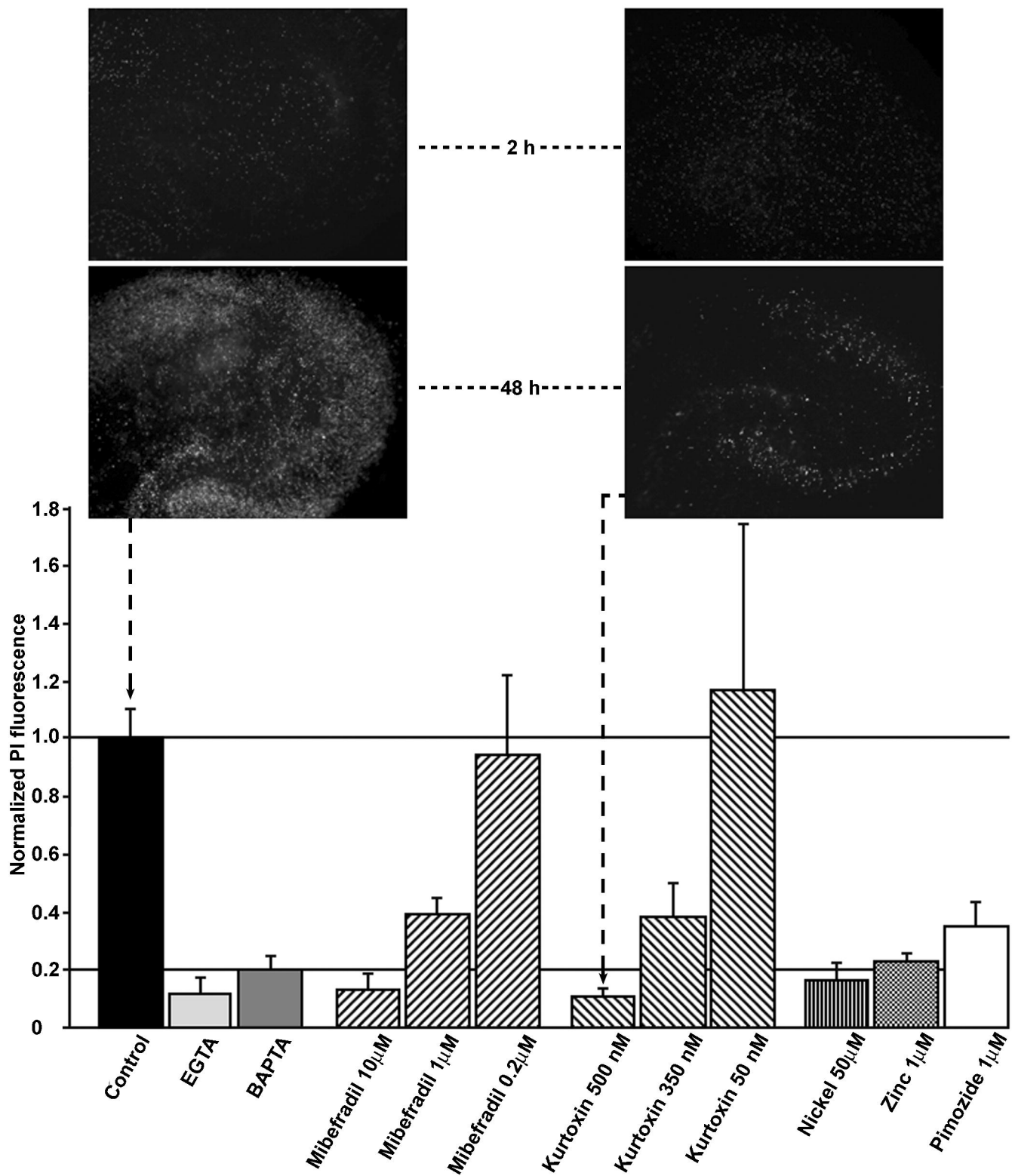


Figure 3

